A Time-Resolved Stimulated Nuclear Polarization Study of Biradicals in Low Magnetic Field

Serguei V. Dvinskikh,[†] Alexandra V. Yurkovskaya,[‡] and Hans-Martin Vieth*,[†]

Institute of Experimental Physics, Free University of Berlin, Arnimallee 14, D-14195 Berlin, Germany, and International Tomography Center, Institutskaya 3a, 630090 Novosibirsk-90, Russia

Received: December 19, 1995; In Final Form: February 22, 1996[⊗]

Stimulated nuclear polarization (SNP) in acyl−alkyl biradicals of different size formed as a result of α-cleavage of cyclic ketones in the triplet state has been investigated in low magnetic field around 10 mT. Time resolution was achieved by pulsing the light and the rf source and monitoring the SNP signal as function of the rf pulse delay. The SNP amplitude reaches its maximum for a delay around 40 ns and decays exponentially for longer delays. The decay time decreases with increasing molecular chain length. The different influence of triplet quencher *cis*-piperylene and radical scavenger $CBrCl_3$ shows that the decay is mainly determined by the lifetime of the photoexcited ketone triplet state. The SNP maximum position can be attributed to the competition between spin-dependent and spin-independent channels of intersystem crossing.

1. Introduction

Spin effects in biradical reactions have been intensively studied for many years. Investigations of chemically induced dynamic electron and nuclear polarizations (CIDEP and CIDNP) have provided detailed information on the kinetics and the mechanism of such reactions. Recent development of time-resolved versions of CIDNP[1] and stimulated nuclear polarization[2] (SNP) methods as well as of time-resolved EPR spectroscopy[3] and pulse mode product-yield-detected ESR (PYESR)[4] made it possible to observe the time evolution of spin effects in highly unstable intermediates with a temporal resolution in the range of 40−100 ns. At low magnetic field, where spin effects are particularly pronounced, only SNP and PYESR give a sufficiently high detection sensitivity, and for the case of cyclic reaction channels SNP is the only technique for monitoring the reaction kinetics.

In this work we study the low-field time-resolved SNP of acyl−alkyl biradicals, which are formed by α-bond cleavage in a cyclic ketone in the optically excited triplet state.[5] In a low-viscosity solution at room temperature, fast tumbling of molecules suppresses the formation of an initial spin polarization of ketone molecules in the triplet state (known as the triplet mechanism of polarization). Spin polarization mainly arises at the biradical stage of the reaction as a result of magnetic interaction with the external magnetic field, hyperfine interaction, and interactions between radical centers. In biradicals the limited separation of radical centers, which are linked by polymethylene chains, provides a considerable electron exchange interaction J during the biradical lifetime. The crossing of the T_- and S levels at a magnetic field of $B_0 = 2|J|/(\beta g)$ leads to an efficient channel of singlet−triplet conversion. The chain dynamics, which randomly varies the distance between radical centers, modulates the exchange interaction $J(r)$ and, consequently, affects the rate of triplet−singlet conversion and thus the spin dynamics of biradicals. The main features of continuous wave (CW) SNP in biradicals at low magnetic fields were considered and accounted for by the $T_-\alpha-S\beta$ conversion (α, β are the "spin up" and "spin down" nuclear spin projections, respectively) as the dominating spin-selective channel of the intersystem crossing[6−8] Until now only one attempt to investigate the kinetics of SNP in biradicals was described.[7] In that work, the time-resolved ^{13}C SNP of the carbonyl moiety of the biradical arising during the photolysis of cyclododecanone at 51 mT was measured as a function of the delay between the laser flash and the rising edge of a long radio frequency (rf) pulse. The time resolution was 40 ns. It was suggested that the observed decay time of 200 ns is determined by both the α-cleavage of the excited triplet ketone and the decay of the biradicals themselves. However, in these experiments, the contribution of each process could not be separated. These contributions can be separated if the effective rate of one of the processes is changed by varying the parameters of the intermediates or of the reaction conditions. The triplet−singlet conversion rate is varied by changing the electron exchange interaction J or a relevant hyperfine interaction (hfi) constant; the average value of J strongly depends on the ketone size, while the hfi constants can be changed by substituting protons with deuterons. The effective lifetimes of biradicals or triplet ketone molecules can be treated separately by using biradical scavengers or triplet state quenchers, which trap the corresponding intermediates.

In the present work, the low magnetic field ^1H SNP evolution of the biradicals generated during the photolysis of cycloalkanones of different cycle sizes ($n = 10, 11, 12$) in the presence of a quencher of the triplet state ketone molecules and scavenger of biradicals is investigated to determine the kinetic parameters of SNP formation.

2. Experimental Section

The time-resolved ^1H SNP experiments were performed on a custom-built FT NMR spectrometer (7 T) with detection at 300 MHz and a fast magnetic field cycling using a pneumatic probe-head transfer system previously designed for the investigation of the optical nuclear polarization of molecular crystals.[9] The photochemical reaction was carried out at the low magnetic field of a current-controlled electromagnet. The solution under investigation was irradiated by a Lambda-Physik excimer laser at 308 nm. The laser pulse duration is 10 ns (fwhm), and the energy per pulse is 100 mJ. Laser irradiation for 1−3 s at a pulse repetition frequency of 10−40 Hz was used to create proton polarization, sufficient to give an adequate signal-to-noise ratio. The frequency for pumping electron spin transitions

[†] Free University of Berlin.
[‡] International Tomography Center.
[⊗] Abstract published in *Advance ACS Abstracts,* April 15, 1996.

S0022-3654(95)03769-5 CCC: $12.00

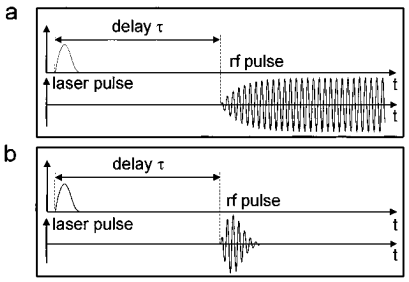

Figure 1. Time diagram of a pulsed SNP experiment: (a) at long rf pulses; (b) at short rf pulses.

was 300 MHz. This allowed us to use the same resonance circuit for high-field proton NMR detection and irradiation of electron spin transitions at low field. The resonance condition for electron pumping was set by adjusting the low magnetic field B_0 to about 11 mT. After irradiation the sample was transferred to the cryomagnet of the spectrometer, where the NMR spectra of polarized products were detected. In time-resolved experiments the delay between the laser flash and the rf pulse was varied. Two types of rf pulses were used: a long pulse ($\sim$2 μs), the duration of which was longer than the SNP decay time ($\sim$0.5 μs) and a short pulse of 15 ns (fwhm) (Figure 1). The experiment with the long rf pulse gives a higher detection sensitivity but has the disadvantage that it detects the integral effect as a response to the total pulse duration; hence, the short pulse can give the SNP time profile in more detail. The rf pulse shape was checked by the signal from a pickup antenna inserted into the probe head. The amplitude B_1 of the rf magnetic field was calibrated by measuring the length of a $\pi/2$ pulse for protons. The time resolution of about 30 ns in experiments with long rf pulses was mainly determined by the duration of the rf pulse edges. In the short-pulse experiments the time resolution of about 20 ns was limited by the duration of the laser and rf pulses; numerical deconvolution allowed us to improve the time resolution to 5 ns. The delay between laser and rf pulse was accurate to 5 ns. In addition, quasi-CW SNP of biradicals was obtained by applying a long rf pulse started before the laser flash in order to measure the resonance condition; also, the B_1 field range, where electron spin coherence effects can be safely neglected, was determined by measuring the SNP dependence on B_1.

The cyclic aliphatic ketones cyclodecanone, cycloundecanone, cyclododecanone ($C_nH_{2(n-1)}O$, n = 10, 11, 12), deuterated chloroform (solvent), bromotrichloromethane (scavenger), and *cis*-piperylene (triplet quencher) were obtained from Aldrich and used as received. Cyclododecanone deuterated in the α-position ($C_{12}D_4H_{18}O$) with the degree of substitution >90% was synthesized according to the technique described.[10] Prior to irradiation, the solutions (0.06 M) were bubbled with argon or helium for 5 min. All experiments were performed at room temperature. The concentration of *cis*-piperylene, which has a low boiling temperature and easily evaporates from the solution, was monitored by the intensity of its NMR signal.

3. Results and Discussion

From a number of investigations of the spin polarization effects,[5,11] it has been established that photoexcitation of cyclic ketones by laser flashes induces the Norrish type I α-cleavage of ketones in their triplet state, which yields triplet biradicals (Scheme 1). After intersystem conversion to the singlet state, biradicals preferentially recombine to the initial ketone molecules.

In acyl−alkyl biradicals, only alkyl end protons exhibit significant hyperfine coupling constants (−2.2 and +2.8 mT for α-CH_2 and β-CH_2, respectively). For all other protons, the hfi constants are below 0.1 mT. We used the hfi constants of the corresponding monoradicals reported in the literature.[12] At low magnetic fields all protons show approximately equal negative polarizations (emission) which are independent of the sign and value of hfi. The feature of uniform polarization of all protons with small hfi due to polarization transfer was analyzed previously; dipolar cross relaxation and spin−spin coupling were considered to be leading mechanisms of redistribution of polarization among the nuclear spins.[13,14] For $C_{12}H_{22}O$ the emission maximum in the CIDNP field dependence is at B_{max} = 15 mT, which is close to the applied magnetic field B_0 = 11 mT, while for $C_{11}H_{20}O$ and $C_{10}H_{18}O$ emission is maximum at 22 and 80 mT, respectively.[11] Therefore, the $T_-\alpha-S\beta$ transitions, important for SNP formation, are expected to be most pronounced for $C_{12}H_{22}O$.

SCHEME 1

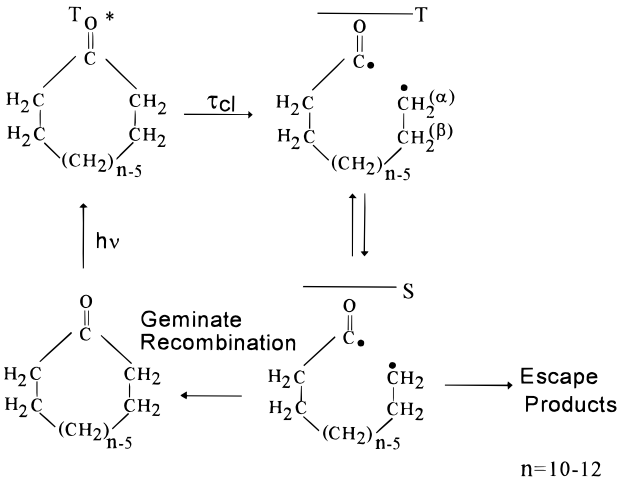

To compare the effects of rf pumping on different samples, we used the value K_{SNP} defined as the normalized difference of CIDNP intensity with and without rf pumping ($I_s - I_c$) with allowance for the "dark" magnetization, I_d, that appeared during sample transfer time due to nuclear spin−lattice relaxation:

$$K_{SNP} = (I_s - I_c)/(I_c - I_d) \quad (1)$$

K_{SNP} describes the relative change of chemical spin polarization due to rf pumping and is independent of sample transfer time, intensity, and duration of laser irradiation. K_{SNP} was measured separately for α-CH_2 protons, β-CH_2 protons, and the unresolved signal of all other protons in the cyclic ketone molecules (below referred to as γ-protons).

3.1. Quasi-CW SNP. For quasi-CW rf irradiation (with long rf pulses starting before the laser flash), the SNP effects observed in our experiments are qualitatively in accordance with existing results.[7] At small B_1 amplitudes all protons show approximately equal positive values of K_{SNP}. The only exception is the value of K_{SNP} for the α-protons, which is slightly higher. The dependences of CW SNP on B_1 show a maximum K_{SNP} of about 0.6 at B_1 = 2.0 mT for $C_{12}H_{22}O$ and of 0.4 at B_1 = 3.0 mT for $C_{11}H_{20}O$ (see Figure 2). For $C_{10}H_{22}O$ the value of K_{SNP} is below 0.1 in the whole B_1 range studied. The decrease of K_{SNP} at high B_1 can be accounted for by strong rf-induced mixing of triplet sublevels. Up to moderately strong B_1 fields (B_1 < 5mT), the observed K_{SNP} value is highest for $C_{12}H_{22}O$. This is not surprising, since, according to the standard perturbation theory, the intersystem crossing rate is proportional to $(V_{TS})^2/((V_{TS})^2 + (E_{TS})^2)$, where V_{TS} is the matrix element of T−S mixing, and E_{TS} is the energy gap between T_- and S levels. Since under

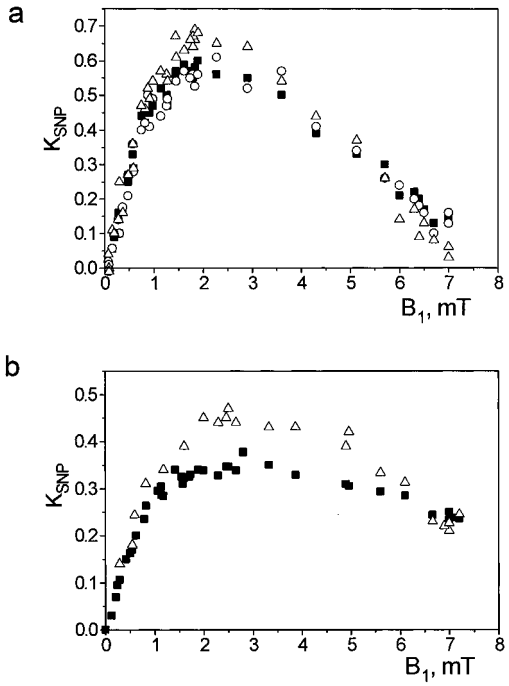

Figure 2. Dependence of K_{SNP} on the rf field amplitude B_1 (CW irradiation): (a) in $C_{12}H_{22}O$ and (b) in $C_{11}H_{20}O$ as detected by NMR signals of α-CH_2 (△), β- CH_2 (○), and γ-CH_2 protons (■).

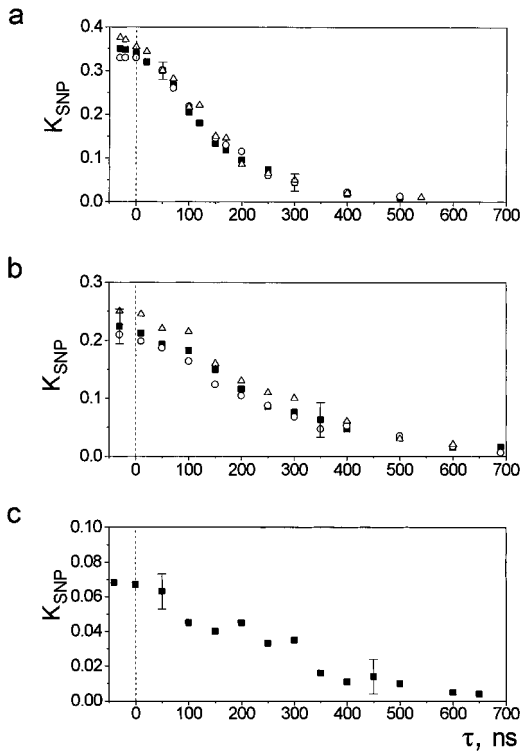

Figure 3. K_{SNP} dependences on the delay τ between the laser flash and the long rf pulse in ketones with different lengths n as detected by NMR signals of α-CH_2 (△), β-CH_2 (○), and γ-CH_2 protons (■): (a) $n = 12$; (b) $n = 11$; (c) $n = 10$.

our experimental conditions ($B_0 = 11$ mT) E_{TS} is smallest for cyclododecanone, it leads to the largest difference of population in the triplet manifold for this compound and, as a consequence, to the highest value of K_{SNP}.

3.2. Time-Resolved SNP. *3.2.1. SNP for Long rf Pulses.* Time-resolved SNP experiments with long rf pulses (2 μs, see Figure 1a) were carried out at $B_1 = 0.6$ mT; at this field all coherences can be neglected. The dependences of K_{SNP} on the delay between the laser flash and the beginning of the rf pulse are shown in Figure 3 for ketones of different sizes. For all proton positions in ketones with $n = 11$ and 12, the SNP time dependences coincide within the margins of experimental error (Figure 3a,b). For $C_{10}H_{18}O$, which shows a weak SNP, K_{SNP} has been measured only for the γ-line of the NMR spectrum, since this line has the highest intensity (Figure 3c). Deuteration of cyclododecanone in its α-position did not show any measurable effect.

Qualitatively, the observed proton SNP decay for $C_{12}H_{22}O$ is similar to the SNP decay of the carbonyl ^{13}C nucleus as measured for the same ketone at $B_0 = 51.0$ mT.[7] For a quantitative comparison, however, the signal-to-noise ratio of the ^{13}C data in ref 7 is too low. The observed SNP decay becomes faster with the increase of the ketone chain length. This tendency is consistent with the results of optical measurements of the lifetime of acyl−phenyl biradicals with long chains at fixed B_0.[15,16] Qualitatively, it can be accounted for by the larger triplet−singlet energy gap for short-chain ketones (at the applied magnetic field of 11 mT). At $B_{max} = 2|J|/(\beta g)$ the $T_- - S$ crossing gives a local maximum of the rate of hfi-induced intersystem conversion.[15b] The position of maximum is closest to the resonance B_0 field for cyclododecanone. For α-substituted cycloalkanones with a cycle length of $n = 10-12$, the literature values of the optically measured biradical lifetimes range between 50 and 200 ns,[15] which is of the same order of magnitude as the SNP decay times observed in this work. On the other hand, the SNP decay time can be accounted for by the time of α-cleavage of the initial ketone in the triplet state, which for the unsubstituted species is in the same range. The lifetime of the photoexcited cyclododecanone in the triplet state, calculated from the Stern−Volmer dependences of the reaction quantum yield[17] and high-field CIDNP intensity[18] versus *cis*-piperylene (triplet quencher) concentration is 170 ns. Thus, in principle, both the α-cleavage of the excited triplet ketone and the biradical lifetime can be limiting stages of the SNP decay. To distinguish experimentally between the contributions of these two factors, we investigated the influence of both $CBrCl_3$, a radical scavenger, and *cis*-piperylene, a quencher of the triplet ketone, which selectively affect the effective lifetime of the corresponding intermediates and the kinetics and the amplitude of SNP.

3.2.1.1. SNP in the Presence of $CBrCl_3$. An important role of the scavenger molecules in the formation of geminate CIDNP is to trap biradicals and therefore to prevent the geminate recombination or disproportionation of biradicals, disregarding their nuclear and electron spin projections. The reaction of an alkyl−acyl biradical with a $CBrCl_3$ molecule proceeds through attachment of the Br atom to one of the biradical ends (Scheme 2). As a result, two types of radical pairs with uncorrelated electron spins appear. A detailed analysis of the NMR spectra of the reaction products has shown preferential attachment of the Br atom to the acyl end of the biradical. Therefore, only this part of the reaction is shown in Scheme 2.

Figure 4a,b shows the SNP time dependences for the β-CH_2 protons of cyclododecanone and cycloundecanone at different concentrations of $CBrCl_3$ (as a radical scavenger). The main effect is the reduction of the initial value of $K_{SNP}(t=0)$ with increasing scavenger concentration. The decay time also slightly decreases. However, these values are much less sensitive to the addition of $CBrCl_3$ than the intensity of CIDNP, whose field dependence in the presence of $CBrCl_3$ was investigated in a previous paper.[19] The effect of $CBrCl_3$ addition on the SNP decay is much lower than would be expected if the biradical lifetime were a bottleneck. Indeed, on the assumption that the scavenger reaction is a pseudo-first-order process and is

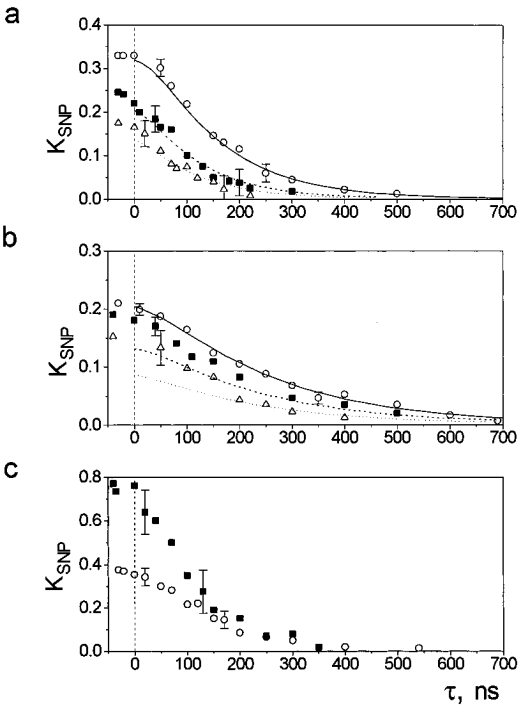

Figure 4. Time dependence of K_{SNP} at different concentrations c_s of scavenger $CBrCl_3$. Lines represent simulations with parameters as explained in the text. (a) β-CH_2 protons of $C_{12}H_{22}O$: ○ (—) $c_s = 0$ M; ■ (- - -) $c_s = 0.01$ M; △ (•••) $c_s = 0.02$ M. (b) β-CH_2 protons of $C_{11}H_{20}O$: ○ (—) $c_s = 0$ M; ■ (- - -) $c_s = 0.005$ M; △ (•••) $c_s = 0.01$ M. (c) α-CH_2 protons of $C_{12}H_{22}O$: ○ $c_s = 0$ M; ■ $c_s = 0.01$ M.

SCHEME 2

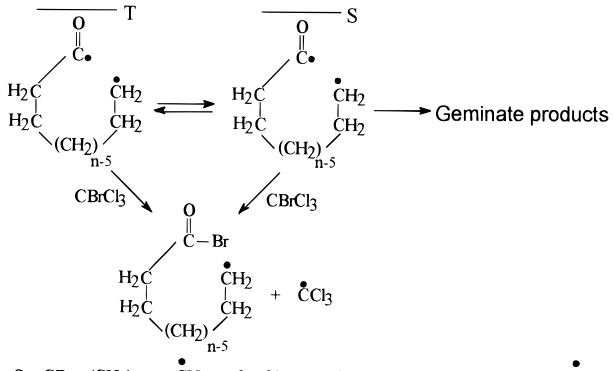

described by an exponential decay with a characteristic time $\tau_s = k_s^{-1}c_s^{-1}$ (k_s and c_s are the reaction rate and scavenger concentration, respectively), the effective lifetime of the biradical in the presence of the scavenger can be estimated as $\tau^{-1} = \tau_0^{-1} + c_s k_s$, where τ_0^{-1} is the biradical lifetime without the scavenger.[19] The reaction rate calculated using the experimental data from Figure 4a,b is $k_s \approx 0.2 \times 10^{-9}$ M^{-1} s^{-1}, which is several times less than the value $(1.0-2.3) \times 10^{-9}$ M^{-1} s^{-1} obtained in refs 19 and 20.

The time dependence of K_{SNP} for γ-protons coincides with that for β-CH_2 within the experimental error. Unlike for β- and γ-protons, for α-CH_2 a significant increase of K_{SNP} was observed, when the scavenger was added (Figure 4c). The CIDNP dependence on the concentration of $CBrCl_3$ observed for α-CH_2 protons was also different from the corresponding dependences for the other proton positions.[19] For α-CH_2 the

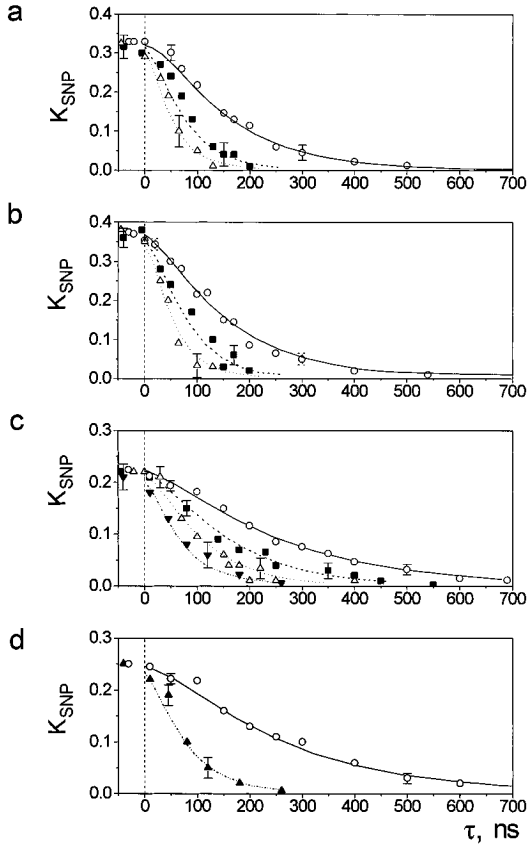

Figure 5. Time dependence of K_{SNP} at different concentrations c_q of quencher *cis*-piperylene. Lines represent simulations with parameters as explained in text. (a) β-CH_2 protons of $C_{12}H_{22}O$: ○ (—) $c_q = 0$ M; ■ (- - -) $c_q = 0.004$ M; △ (•••) $c_q = 0.008$ M. (b) α-CH_2 protons of $C_{12}H_{22}O$: ○ (—) $c_q = 0$ M; ■ (- - -) $c_q = 0.004$ M; △ (•••) $c_q = 0.008$ M. (c) γ-CH_2 protons of $C_{11}H_{20}O$: ○ (—) $c_q = 0$ M; ■ (- - -) $c_q = 0.0005$ M; △ (•••) $c_q = 0.001$ M; ▼ (—••—) $c_q = 0.005$ M. (d) α-CH_2 protons of $C_{11}H_{20}O$: ○ (—) $c_q = 0$ M; ▲ (—••—) $c_q = 0.005$ M.

CIDNP intensity decreased rapidly by addition of the scavenger and the sign of the polarization changed from emission to absorption at high $CBrCl_3$ concentrations, while the other protons showed emission at all concentrations of $CBrCl_3$. This behavior was accounted for by relative increase in the contribution from $S-T_0$ transitions. This contribution depends on the sign of the hfi constant and should give an absorptive line for α-CH_2. We attribute the relative increase of SNP for α-CH_2 to the same reason. For α-CH_2, K_{SNP} is higher, since the CIDNP signal is lower (see eq 1).

3.2.1.2. SNP in the Presence of cis-piperylene. Unlike bromotrichloromethane, which affects only biradicals, *cis*-piperylene effectively quenches the triplet state of ketone molecules at a rate close to the diffusion rate but has no influence on biradical states.[17] Addition of *cis*-piperylene to the solution (up to 0.005 M) leads to a strong decrease of the SNP decay time (Figure 5). On the other hand, the addition of *cis*-piperylene unlike the addition of $CBrCl_3$ does not change the initial value $K_{SNP}(t=0)$. This result can be accounted for by the fact that the biradical stage of the reaction, when the SNP effect is formed, is insensitive to the addition of *cis*-piperylene. Further increase in *cis*-piperylene concentration (>0.01 M for cyclododecanone and >0.005 M for cycloundecanone) does not change the amplitude and time profile of K_{SNP}. Such a saturation is expected if the effective lifetime of the triplet ketone becomes shorter than the time of the biradical decay and the latter is the slowest process which limits the SNP decay rate. Therefore, the average lifetime of the biradical can be estimated from the SNP decay time at high *cis*-piperylene

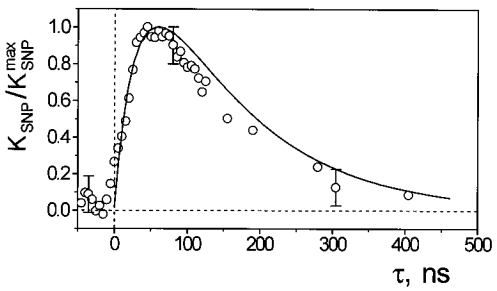

Figure 6. K_{SNP} (normalized with respect to the value at maximum) as function of the delay between laser flash and short rf pulse for α-CH_2 protons in $C_{12}H_{22}O$. The solid line represents the model calculation with parameters as explained in the text.

concentrations; it is 80 ns for cycloundecanone and 50 ns for cyclododecanone. These values are comparable with literature data reported for similar species in low-viscosity solutions.[15,16] On the other hand, in the absence of quencher, the decay time is determined mainly by the lifetime of the triplet state of the photoexcited ketone, which can be estimated as 250 ns in $C_{11}H_{20}O$ and 150 ns in $C_{12}H_{22}O$.

3.2.2. SNP for Short rf Pulses. For a more detailed analysis of the SNP evolution during the reaction, we carried out additional time-resolved SNP experiments using short rf pulses (15 ns fwhm) with a maximum B_1 value of 0.7 mT. These experiments allowed us to observe the SNP kinetics at short delay times after the laser pulse. The results for the α-CH_2 protons of $C_{12}H_{22}O$ are shown in Figure 6, where the circles represent the experimental points after deconvolution with respect to the shapes of the rf and laser pulses. In principle, the standard deconvolution method can be applied only if the response is linear, which is not necessarily fulfilled in the case of our experiments because of coherence effects imposed on the spin system by the strong rf pulse. The linearity was checked in two different ways. The dependence of K_{SNP} on the area of the rf pulse was measured and did not show significant nonlinearity under variation of the B_1 amplitude and the pulse length in the ranges of 0−1.0 mT and 10−50 ns, respectively. Moreover, the deconvolution of the time profile of K_{SNP}, which was measured by rf pulses of different length (15, 25, and 40 ns (fwhm)), gives approximately the same shape with the amplitude increasing proportionally to the pulse area. As can be seen from Figure 6, the K_{SNP} signal initially rises, and the intensity is maximum at a delay of about 40 ns after the laser flash. Then the signal slowly decays, with a time constant equal to that observed under irradiation by long rf pulses. Immediately after the laser pulse the rf pumping does not affect the CIDNP intensity (i.e. $K_{SNP} = 0$), since the lifetime of the triplet state of the ketone is finite and the populations of the triplet sublevels are assumed to be equal. Instead the rise time of K_{SNP} is determined by the difference of the spin-dependent depopulation rates of the biradical triplet sublevels. The slow formation of the biradical from the precursor is expected to mask this process, thus leading to a slower increase in K_{SNP}. The position and magnitude of the K_{SNP} maximum can be related to the competition with spin-independent processes such as electronic relaxation and spin−orbit coupling, which tend to equalize the populations of the triplet sublevels. The small positive initial value of K_{SNP} can, in principle, be accounted for by a weak contribution of the triplet mechanism to the formation of the polarization.[21]

3.3. Model Calculation. Below we consider a simple kinetic scheme based on a system of rate equations to simulate the SNP time evolution. The model is in many respects analogous to the approach developed to interpret the time-resolved EPR of radical pairs in micelles.[22] The bond cleavage in a triplet ketone with rate k_{cl} initially yields biradicals with pure triplet spin character. Magnetic hyperfine and spin−orbit interaction lead to different degrees of quantum mechanical mixing of singlet and triplet character for the biradical eigenstates with a dependence on the nuclear spin orientation. For the calculation two groups of protons from the alkyl end, α-CH_2 and β-CH_2, are taken into account with hyperfine coupling constants of −2.2 and 2.8 mT, respectively. The result is selective population proportional to the triplet character. A possible, small contribution from spin polarization of the precursor triplet is neglected, as well as the Boltzmann polarization. It is assumed that the mixing occurs faster than does the biradical decay. The effective rate of ground state ketone formation from each biradical state is proportional to its singlet character λ_i and to the rate of recombination from the pure singlet state, which is supposed to be equal to the end-to-end re-encounter rate k_r. Electron relaxation due to the fluctuation of local magnetic fields is taken into account.[5] The correlated relaxation due to fluctuations of the dipole−dipole interaction is neglected, since the corresponding rate, estimated using the distance distribution of the paired radical centers and a realistic correlation time around 10^{-11} s, is negligible: $R \sim 4 \times 10^5\ s^{-1}$.[5] The spin-independent channel of the intersystem crossing by spin−orbit coupling at a rate k_{soc} is taken into account.

In the calculation, the scavenger reaction rate and the rate of quenching by *cis*-piperylene were taken as $k_s = 2.3 \times 10^9\ M^{-1}\ s^{-1}$ [19] and $k_q = 6.0 \times 10^9\ M^{-1}\ s^{-1}$, [17,23] respectively. The rate of end-to-end reencounter $k_r = 10^{10}\ s^{-1}$ was taken from literature.[3,24] The value of exchange integral J taken as a weighted average over all molecular conformations was estimated from the condition $g\beta B_{max} = 2|J|$, where B_{max} corresponds to the experimentally observed position of the maximum of the CIDNP field dependence. The rate of α-cleavage, k_{cl}, the rate of intersystem conversion via spin−orbit coupling, k_{soc}, and the relaxation rate k_{rel} were adjusted for the best fit. However, only k_{cl} can be determined with a good accuracy, while each of the values of k_{soc} and k_{rel} can be varied over 1 order of magnitude, from 10^6 to $10^7\ s^{-1}$, with strong correlation between each other by the condition that their sum is approximately constant ($k_{soc} + k_{rel} \sim 10^7\ s^{-1}$).

The SNP decay curves obtained in the presence of *cis*-piperylene fit very well in terms of this model (Figure 5). Also, the measurements for the biradical scavenger $CBrCl_3$ can be explained at least qualitatively (Figure 4) in accordance with literature data. For the curves given in Figures 4 and 5, the parameters of the model are as follows: $k_{cl} = 7.5 \times 10^6\ s^{-1}$ and $k_{cl} = 4.5 \times 10^6\ s^{-1}$ for $C_{12}H_{22}O$ and $C_{11}H_{20}O$, respectively, and $k_{soc} = 3 \times 10^6\ s^{-1}$ and $k_{rel} = 8 \times 10^6\ s^{-1}$ for both ketones.

The present model seems to be too crude to correctly describe the short-time SNP kinetics, since the assumption of the instantaneous mixing of states fails in this regime. Nevertheless, the time profile of SNP at short rf pulses was calculated in terms of the same model with the parameters obtained by simulating the experiments with long rf pulses. The results are in agreement with the deconvoluted experimental data (Figure 6). Variation of the model parameters shows that the rise time (at fixed rate k_{cl}) is mainly affected by the recombination rate. The rate k_{soc} slightly shifts the maximum position, and both k_{soc} and k_{rel} affect the maximum amplitude of K_{SNP}. It was found that for values of k_r below $2 \times 10^9\ s^{-1}$ or above $3 \times 10^{10}\ s^{-1}$ the experimental data cannot be simulated within the frame of the model even when the regime of allowed k_{rel} and k_{soc} values is strongly increased.

Despite the surprisingly good fit, the physical significance of the resulting parameters has to be considered with caution because of the obvious shortcomings of the model. More elaborate theories on the interplay between molecular mobility and spin motion have to be applied. In particular it will be interesting to compare the SNP kinetics at different conditions of state mixing. Therefore, experiments are in progress to measure the SNP kinetics at different magnetic fields as well as for other nuclear isotopes.

4. Conclusion

In conclusion, it can be stated that the pulsed SNP method described here, which combines temporal resolution on the EPR time scale and spectral resolution of high-field NMR, allows the investigation of the spin polarization dynamics in biradical reactions in low magnetic field with time resolution of a few nanoseconds. The kinetic parameters of precursor states and biradicals can be separately determined from the SNP time evolution in a much more direct way than can be done using standard CW techniques. Since K_{SNP} measures the SNP effect relative to the corresponding CIDNP signal, it is independent of experimental parameters such as light intensity, sample volume, etc. and can thus be used to compare different compounds or different reaction conditions.

For medium size unsubstituted acyl−alkyl biradicals at low magnetic fields, the SNP decay time is mainly determined by the rate of α-cleavage in the photoexcited triplet state of the ketone. This rate increases with the length of the poly(methylene)chain. The experiments with short rf pulses give additional information on the initial SNP kinetics. The observed maximum of the SNP time dependence at a delay of 40 ns after the laser flash can be attributed to the competition between spin-dependent and spin-independent channels of the biradical triplet−singlet intersystem conversion.

Acknowledgment. The authors are grateful to M. Benkert and A. Privalov for technical assistance in the modification of the experimental setup. Financial support from the Deutsche Forschungsgemeinschaft (Sfb 337) is gratefully acknowledged. A.Y. thanks the International Science Foundation (project JJD 100) for additional support.

References and Notes

(1) Miller, R. J.; Closs, G. L. *Rev. Sci. Instrum.* **1981**, *52*, 1876.

(2) Bagryanskaya, E. G.; Sagdeev, R. Z. *Prog. React. Kinet*. **1993**, *18*, 63.

(3) Closs, G. L.; Forbes, M. D. E. *J. Am. Chem. Soc*. **1987**, *109*, 6185.

(4) (a) Okazaki, M; Toriyama, K. *Bull. Chem. Soc. Jpn*. **1993**, *66*, 1892. (b) Okazaki, M.; Polyakov, N.; Konishi, Y.; Toriyama, K. *Appl. Magn. Reson*. **1994**, *7*, 49.

(5) de Kanter, F. J. J.; den Hollander, J. A.; Huizer, A. H.; Kaptein, R. *Mol. Phys*. **1977**, *34*, 857.

(6) Koptyug, I. V.; Bagryanskaya, E. G.; Sagdeev, R. Z. *Chem. Phys. Lett*. **1989**, *163*, 503.

(7) Koptyug, I. V.; Bagryanskaya, E. G.; Grishin, Yu. A.; Sagdeev, R. Z. *Chem. Phys.* **1990**, *145*, 375.

(8) Koptyug, I. V.; Lukzen, N. N.; Bagryanskaya, E. G.; Doctorov, A. B.; Sagdeev, R. Z. *Chem. Phys*. **1992**, *162*, 165.

(9) Allgeier, J.; Buntkowsky, G.; Hentrich, S.; Nack, M.; Vieth, H.-M. *Ber. Bunsen-Ges. Phys. Chem.* **1989**, *93*, 1281.

(10) Murray, A.; Williams, D. L. *Organic Syntheses with Isotopes;* Interscience: New York, 1958; Vol. 2.

(11) Closs, G. L. *Adv. Magn. Reson*. **1974**, *7*, 157.

(12) *Landolt-Börnstein, Magnetic Properties of Free Radicals*; Fischer, H., Ed.; New Series, Springer: Berlin, 1980**;** Vol. II 9, b, pp 15−21.

(13) de Kanter, F. J. J.; Kaptein, R. *J. Am. Chem. Soc*. **1972**, *94*, 6269.

(14) Tarasov, V. F.; Shkrob, I. A. *J. Magn. Reson. A* **1994**, *109*, 65.

(15) (a) Zimmt, M. B.; Doubleday, C., Jr.; Gould, I. R.; Turro, N. J. *J. Am. Chem. Soc.* **1985**, *107*, 6724. (b) Zimmt, M. B.; Doubleday, C., Jr.; Turro, N. J. *J. Am. Chem. Soc*. **1985**, *107*, 6726 . (c) Zimmt, M. B.; Doubleday Jr., C.; Turro, N. J. *J. Am. Chem. Soc*. **1986**, *108*, 3618. (d) Wang, J.; Doubleday, C., Jr.; Turro, N. J. *J. Am. Chem. Soc.* **1989**, *111*, 3962. (e) Wang, J.-F.; Rao, V. P.; Doubleday C., Jr.; Turro, N. J. *J. Phys. Chem*. **1990**, *94*, 1144.

(16) Johnston, L. J.; Scaiano, J. C. *Chem. Rev.* **1989**, *89*, 521.

(17) Burchill, P. J.; Kelso, A. G.; Power, A. J. *Aust. J. Chem*. **1976**, *29*, 2477.

(18) Tsentalovich, Yu. P.; Yurkovskaya, A. V.; Sagdeev, R. Z. *J. Photochem. Photobiol. A* **1993**, *70*, 9.

(19) Yurkovskaya, A. V.; Morozova, O. B.; Sagdeev, R. Z.; Dvinskikh, S. V.; Buntkowsky, G.; Vieth, H.-M. *Chem. Phys.* **1995**, *197*, 157.

(20) (a) Hwang, K. C.; Turro, N. J.; Doubleday, C., Jr. *J. Am. Chem. Soc.* **1991**, *113*, 2850. (b) Turro, N. J.; Hwang, K. C.; Rao, V. P.; Doubleday C., Jr. *J. Phys. Chem.* **1991**, *95*, 1872.

(21) Wan, J. K. S.; Depew M. C. *Res. Chem. Intermed.* **1992**, *18*, 227.

(22) Closs, G. L.; Forbes, M. D. E.; Norris, J. R., Jr. *J. Phys.Chem*. **1987**, *91*, 3592.

(23) Dalton, J. C.; Turro, N. J. *Annu. Rev. Phys. Chem.* **1970**, *21*, 499.

(24) Forbes, M. D. E. *J. Phys. Chem.* **1993**, *97*, 3390.

JP953769K